Electrospun light-emitting nanofibers as excitation source in microfluidic devices

Stefano Pagliara,[ab] Andrea Camposeo,[a] Alessandro Polini,[ab] Roberto Cingolani[a] and Dario Pisignano*[ab]

Received 27th March 2009, Accepted 18th June 2009
First published as an Advance Article on the web 7th July 2009
DOI: 10.1039/b906188f

We introduce the integration of organic, polarised light-emitting electrospun nanofibers and lab-on-a-chip microchannel geometries. The alignment and spinning electric field leads to ordered mesoscopic active areas, up to many mm^2, which exhibit polarised light emission and are fully compatible with microlithographies and microfluidics. We utilise the nanofibers demonstrating the photo-excitation of flowing dye chromophores in microchannels. This leads to easy decoupling the excitation and sample emission by polarisation analysers, thus remarkably increasing the imaging signal to background noise ratio.

Introduction

Active organic one-dimensional (1D) nanostructures are particularly attractive as low-cost sources of polarised light.[1] In particular, realising and characterising miniaturised light-emitting sources is crucial for many lab-on-a-chip applications. To date, most of these devices had to be connected to external light sources (lamps, light-emitting diodes, and lasers) for exciting chromophore fluorescence. The demonstration of photoluminescence (PL) from novel, miniaturisable organic nanostructures embedded or coupled to microchannels is an important step towards the realization of electroluminescent devices, which would ultimately guarantee compact integration into microfluidic devices and enhanced portability.

Importantly, for high-sensitivity diagnostic applications, one should also mention the tiny liquid volumes and the low analyte–antigen concentrations, rendering the availability of polarised light sources very desirable for integration into lab-on-chips. In fact, commonly employed photo-excitation is up to orders of magnitude more intense than the detected PL of chromophores flowing or immobilised within microchannels. Optical filtering of the excitation light is generally a particularly critical issue limiting the overall sensitivity.[2] Previously reported approaches to partially overcome this problem include directional coupling of excitation photons into microchannels by means of fiber optics, whose path can be carefully controlled and spatially separated from the detection area.[2] Miniaturised polarisers for external UV or visible excitation light such as wire grid polarisers require technologically-demanding, often expensive lithographies with sub-wavelength resolution capability.[3] Integrated, polarised organic light-sources would instead enable low-cost and easy decoupling of excitation and fluorescence signals.

Very recently, a few pioneering experiments have been performed on device-integrated fluorescence pumping in microscale capillaries,[4–7] mainly focused on unpolarised polymer light-emitting diodes (PLEDs). Here we report on the integration of photo-excited, aligned organic nanofibers as polarised, nano- to mesoscale light sources in a prototypical microchannel geometry for lab-on-a-chip architectures. We also relate the achievable degree of mutual alignment of fibers, and the resulting optical anisotropy, to the alignment electric field and geometry. Finally, by means of the aligned light sources, we excite flowing chromophore molecules. The nanofibers absorb a part of an external laser light and re-emit polarised light at a different frequency, and in turn the fluorophores absorb and re-emit light isotropically. This allows us to easy decouple the sample emission from the excitation signal, and to increase the imaging signal/excitation background (S/N) ratio.

The principle behind this approach is simple (Fig. 1): Due to the electrospinning (ES) electric fields (generally related to both the applied anode–cathode bias and electric charges on the collector electrodes), polymer backbones within a single polymer nanofiber orient preferentially along the longitudinal fiber axis, as demonstrated by infrared absorption and Raman spectroscopy.[8–10] By

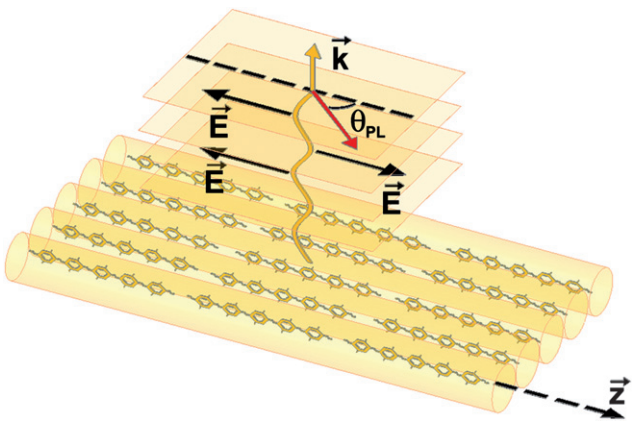

Fig. 1 Polarised light-emitting nanofiber mechanisms. **k** and θ_{PL} indicate the direction of light propagation (yellow arrow) and the angle between the polarisation analyser direction (red arrow) and the longitudinal axis (**z**) of the nanofibers in the array. **E**: electric field vectors.

[a]*NNL, National Nanotechnology Laboratory of CNR-INFM, Università del Salento c/o Distretto Tecnologico,* via *Arnesano, I-73100 Lecce, Italy. E-mail: Dario.pisignano@unile.it; Fax: +39 0832298146; Tel: +39 0832298146*
[b]*Scuola Superiore ISUFI, Università del Salento,* via *Arnesano, I-73100 Lecce, Italy*

means of patterned metallic collectors,[11] many (in the range of 10^3–10^4) nanofibers can in turn be mutually aligned in order to form active areas (up to many mm^2), fully integrable within microfluidic devices. Oriented chains of light-emitted polymers preferentially emit light polarised along their backbone axis, this approach thus lead to the realisation of polarised light sources.

Experimental

Materials

The light-emitting conjugated polymer poly[2-methoxy,5-(2-ethylhexyloxy)-phenylene-vinylene] (MEH-PPV, American Dye Source Inc., Baie-d'Urfé, Canada) used in this study has a molecular weight of about 374 000 Da and it is dissolved in 1,2-dichloroethane (J. T. Baker, Phillipsburg, NJ). The polymeric host matrix is poly(methylmethacrylate) (PMMA, Sigma-Aldrich, St Louis, MO) with a molecular weight of 120 000 Da and it is dissolved in formic acid (Fluka, Buchs, Switzerland) or in 1,2-dichloroethane. The dye Rhodamine 6G (R6G, molecular weight of 480 Da, Sigma-Aldrich, St Louis, MO) is dissolved in ethanol (Fluka).

Electrostatic spinning

ES is performed by placing about 0.5 ml of solution into a 1.0 mL plastic syringe tipped with a 23-gauge stainless steel needle. The positive lead from a high voltage supply (XRM30P, Gamma High Voltage Research Inc., Ormond Beach, FL) is connected to the metal needle applying a bias in the range 7.5–15.0 kV. The solution is injected at the end of the needle at a constant rate of 10 μL/min by a syringe pump (33 Dual Syringe Pump, Harvard Apparatus Inc., Holliston, MA), which prevents dripping at the end of the metallic capillary. Aligned arrays of fibers are obtained by using as collector a 1 mm-thick copper foil with rectangular gaps of different width (1, 1.5 or 2 mm as shorter side). The foil is placed at a distance of 12 cm from the needle and employed over a collection time kept fixed at 6 minutes. The concentration, C, of the host polymer in formic acid is optimised in the range 20–30% (w/w), finding that $C = 30\%$ leads one to obtain too viscous solutions that can not be electrospun, whereas using $C = 20\%$ results in a remarkable presence of beads among fibers, possibly deteriorating the resulting array optical anisotropy. A similar procedure is employed to experimentally determine the optimised concentration of MEH-PPV/PMMA blend in 1,2-dichloroethane. All the ES experiments are performed at room temperature with air humidity about 40%.

Microfluidics

Master structures employed for templating the poly(dimethylsiloxane) (PDMS) elements are fabricated by photolithography. After the deposition of standard photoresist (AZ5214E:AZ EBR Solvent 1:1, AZ Electronic Materials, Wiesbaden, Germany), UV-exposure (20 seconds at 350 W) and development, we etch the thermal dioxide by using $NH_4F/HF/H_2O$ (6.6g/1.6ml/10ml). The so obtained SiO_2 mask is then employed to etch Silicon by 5.9 M solutions of KOH at 110 °C. Monocrystalline (100) Silicon samples are etched along {111} walls inclined at 54° with respect to the bottom of the microchannels. The elastomeric replicas are then obtained by *in situ* polymerisation (75 °C, 15 minutes) of PDMS (Sylgard 184 by Dow Corning, Midland, MI, A:B 1:9). The microchannels (height ≅ 5.0 μm, width ≅ 100 μm, and length ≅ 10 mm) are defined by the superposition of the patterned PDMS element and a bottom flat substrate of PDMS or quartz, by means of bonding or conformal contact. Once this microfluidic device is assembled, the microchannel is aligned over the gap of the copper foil collector supporting the nanofibers. The bottom of the device is then placed in contact with the Cu foil by hand. In this way, the suspended nanofibers are perpendicular to the microchannel long axis, directly in front of the capillary, and separated from the flowing liquid by the transparent (PDMS or quartz) bottom layer of the microfluidic device. The flow rate of 50 μM R6G solution in ethanol, which is then letting to penetrate into the microchannels by spontaneous capillarity, is measured to be (11 ± 1) mm/s.

Optical characterisation

The polarisation-dependent transmission of nanofibers is studied by a calibrated W lamp as light source, an optical polarisation filter mounted on a rotating stage polarising the light incident onto the sample, and a fiber-coupled monochromator (iHR320, HORIBA Jobin Yvon, Edison, NJ) equipped with a charge coupled device detector (Simphony CCD detection systems, HORIBA, Jobin Yvon) to record transmission spectra. The characterisation of polarised PL is carried out using a laser diode (405 nm) as excitation source. The PL spectrum of the composite nanofibers is found to be different with respect to that of MEH-PPV bare films, since exhibiting a broad peak around 530 nm. As recently reported,[12] the acidic property of pyridinium formate may reduce the number of MEH side-groups, thus producing a blue-shift of the polymer luminescence. For excitation of emitting nanofibers coupled to microchannels, a well-collimated laser beam is directed perpendicularly to the entrance, leg face of a right angle prism (PS908 BK7, Thorlabs, Dachau/Munich, Germany), thus being reflected at nearly the critical angle (41°) condition for total internal reflection (TIR) at the hypotenuse face. The hypotenuse face of the prism is placed directly in contact with the nanofibers underneath the microchannel. About 75% of the evanescent laser light at the prism hyphotenuse is absorbed by the nanofibers. This geometry allows to excite only nanofibers in contact with the prism surface and to use the generated fluorescence for exciting R6G molecules in superimposed microchannels. R6G absorption is measured by a double-beam Cary 5000 spectrophotometer (Varian, Palo Alto, CA). Emission signals from both nanofibers and R6G molecules are collected through the objective (with ×10 magnification) of a microscope (BX52, Olympus, Tokyo, Japan) and a rotating polarisation analyser, and imaged by a Digital Camera (DFC 490, Leica, Wetzlar, Germany).

Results

In a typical ES experiment, we prepare a 2.4 mM blend of MEH-PPV/PMMA with weight : weight relative concentration 2%. The PPV-derivative exhibits a high degree of anisotropy of its molecular emission,[13] and the PMMA matrix favours the formation of bead-free nanofibers uniform in diameter. The host

polymer is first dissolved in formic acid, chosen for its high dielectric constant, which disfavours the formation of beads and reduces the resulting fiber diameter.[14] Optimised, bead-free PMMA fibers are realised by a relative concentration of 26% (w/w) in formic acid, with average diameter of (260 ± 40) nm (inset of Fig. 2a). MEH-PPV based fibers are obtained by a concentration of the polymeric blend of 20% in 1,2-dichloroethane, with the addition of 8% (in volume) of pyridinium formate to increase the solution conductivity.

The optical anisotropy of nanofiber arrays is expected to be strongly dependent on the degree of mutual alignment among the fibers. In fact, deposited fibers which are not parallel to the short side of the ES rectangular gaps collector (collector gap axis) are detrimental to the resulting emission polarisation. In order to quantitatively investigate the achieved degree of mutual alignment among the fibers, we approximate each fiber as a segment bridging the collector gap and we measure the angle (α) between each fiber axis and the collector gap axis (highlighted as blue and red line respectively in the inset of Fig. 2a).[11] We find that the resulting angular distribution is well fitted by a Gaussian function:

$$G(\alpha) \sim \exp\left[-\frac{(\alpha-\alpha_0)^2}{2\sigma^2}\right] \quad (1)$$

where α_0 and σ are the mean angle and standard deviation, respectively. By fitting data we typically find an angular distribution well centred around $\alpha_0 = 0°$, with σ in the range 3°–5°, indicating a very high degree of alignment of the fibers in the array. In the following we use, as non-dimensional parameter quantifying the degree of fiber alignment, the quantity: $\psi = \frac{90° - \sigma}{90°}$ ($0 \le \psi \le 1$, with $\psi = 0$ for isotropic orientation and $\psi = 1$ for perfect alignment). The highest alignment, $\psi = (0.92 \pm 0.01)$, is obtained by a particular value of the applied electric field (0.88 kV cm^{-1} for our PMMA system), whereas a decrease of the alignment degree is observed for both lower and higher values of the applied field (Fig. 2a). Upon applying a low electric field, nanofibers are likely to not be sufficiently stretched along the gap, thus being deposited through a wide range of mutual angles. On the contrary, samples realised by a too high electric field (>1 kV cm^{-1}) often exhibit a large number of fibers split into several smaller polymer wires, generally misaligned with respect to the original direction. Moreover, we found that ψ decreases upon increasing the collector gap width. In fact, PMMA nanofibers with diameters in the range 300–500 nm exhibit a quite low Young's modulus (~70 MPa),[15] hence increasing the gap width leads to increasing the number of fibers which bend downward and loose the alignment direction.

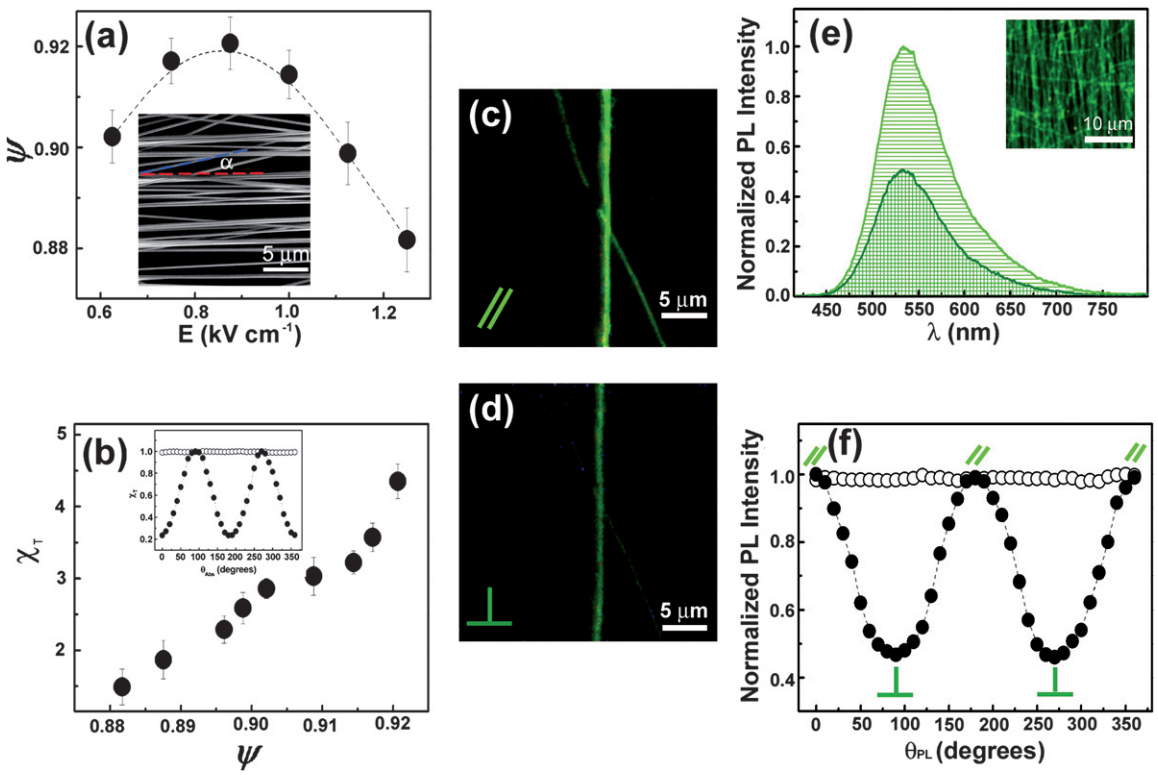

Fig. 2 Influence of the degree of alignment, ψ, of nanofibers on optical properties. (a): ψ *vs.* applied electric field, for PMMA nanofibers. Inset: Typical aligned fiber array. The angle, α, between collector gap axis (red line) and fiber axis (blue line) is displayed for reference. (b): χ_T *vs.* ψ in the array. Inset: Dependence of light transmitted through non woven mats of nanofibers (hollow circles) and aligned arrays (solid circles) on the angle, θ_{Abs}, between the polarisation direction of the incident light and the longitudinal axis of the nanofibers in the array. (c, d): Light-emitting MEH-PPV/PMMA nanofiber micrographs collected with a polarisation analyser oriented parallel (c) and perpendicular (d) to the nanofibers longitudinal axis. (e): Corresponding PL spectra, with analyser parallel (horizontally textured spectrum) and perpendicular (vertically textured spectrum) to the nanofiber axis. Inset: fluorescence micrograph of an aligned array of MEH-PPV based nanofibers. (f): Dependence of the PL emission from non woven mats of nanofibers (hollow circles) and aligned arrays (solid circles) on the angle, θ_{PL}.

To enlighten the correlation between achievable optical anisotropy and inter-fiber alignment degree, we first compare the transmittance of polarised light through aligned arrays and through isotropic non-woven mats of fibers. While not being affected by the incident polarisation for mats, the transmission through arrays shows a significant polarisation dependence, being minimum for incident polarisation parallel to the longitudinal axis of nanofibers ($T_{//}$), and maximum for normal polarisation ($T_{\perp}$). The interaction between electromagnetic radiation and an array of transparent cylindrical objects, having spacing and diameter comparable to the radiation wavelength, is mainly governed by scattering and diffraction, both depending on light polarisation.[16] Fig. 2b shows how the transmission polarisation ratio, $\chi_T = \frac{T_{\perp}}{T_{//}}$, increases upon increasing the alignment degree of nanofibers, up to a maximum value of 4.4 ± 0.2. The inset of Fig. 2b displays the dependence of the transmitted light on the angle (θ_{Abs}) between the polarisation direction of incident light and the longitudinal axis of the fiber array (solid circles), compared with that of an optically isotropic nanofiber-based surface (non-woven mat, hollow circles). The observed behaviour for the aligned array is well described by a squared-sine dependence on θ_{Abs}, whereas the transmission of a non-woven mat of nanofibers is almost independent on the polarization direction of incident light. This confirms the good degree of mutual alignment of the nanofibers in the array. Upon increasing the alignment degree by 4%, χ_T becomes nearly three times larger (Fig. 2b), and a tighter control on the nanofibers alignment,[8,17,18] could lead to a polarisation ratio even larger. Polarised transmittance may open the way for the use of nanofiber arrays as passive optical devices,[19] such as organic ultrathin optical polariser or beam splitters. However, this can hardly be exploited by active, light-emitting nanophotonic devices. For these applications, polarised fluorescence is needed.

In our experiments, emission polarisation is first appreciable in the fluorescence of single fibers, collected through a polarisation analyser (Fig. 2c–d). Furthermore, for aligned arrays of nanofibers (micrograph in the inset of Fig. 2e), the PL spectrum recorded with the analyser oriented parallel to the longitudinal axes of the fibers exhibits a peak in intensity about two times larger than that obtained with the analyser along the orthogonal direction, evidencing polarised emission (horizontally and vertically textured spectra in Fig. 2e, respectively). Fig. 2f displays the normalised PL intensity as a function of the angle (θ_{PL}) between the orientation of the analyser and the longitudinal axis of the aligned nanofibers. Our arrays show a PL polarisation ratio, $\chi_{PL} = \frac{PL_{//}}{PL_{\perp}}$, where $PL_{//}$ ($PL_{\perp}$) is the value of PL intensity with the analyser oriented parallel (perpendicular) to the nanofibers longitudinal axis, of (2.2 ± 0.2), obtained by averaging on the values measured for several (>10) samples. The here found polarisation contrast is similar to that reported for the luminescence of MEH-PPV single molecule spin-cast from toluene solutions,[20,21] exhibiting polarisation ratio of about 2 because of their intrinsic multichromophore nature. It is also comparable to values measured on single, highly-organised 5-nm oligo-(*p*-PPV)-based fibers deposited on graphite.[22]

The polarised light-emitting arrays are then used as excitation sources embedded in microfluidic geometries. To this aim, a PDMS mold is placed on a transparent (polymer or quartz) flat element, and then aligned on a suspended array of organic nanofibers (Fig. 3a). The overall assembly also includes a prism for TIR excitation, on its turn placed in contact with the nanofibers underneath the microchannel, as schematised in Fig. 3a. Fig. 3b shows an optical micrograph of an exemplary microchannel built on a nanofiber light-source, which emits bright green fluorescence (Fig. 3c) upon optical excitation by the evanescent field obtained through TIR of a laser beam in a right angle prism. R6G molecules injected in the microchannels, whose absorption is almost resonant with the nanofiber emissions (Fig. 3d), are excited by the polarised light from the fibers (Fig. 3e), the external laser beam being not collected by the detection system because of the TIR geometry. By rotating a polarisation analyser perpendicularly to the nanofibers longitudinal axis, the unpolarised fluorescence signal from the R6G chromophore solution remains almost unchanged, while the signal from the nanofiber array is drastically reduced (Fig. 3f). This results in an increase of the S/N ratio by about a factor two (Fig. 3g,h).

To date, the use of electrospun nanofibers within microfluidic devices has been mainly limited to solid supports of high surface area for working as filtration membranes[23] or promoting the adsorption of immunoassay antibodies.[24] When compared to existing methods for sensing and detection,[25] relying on filtering, spectrally-sensitive photodetection, or on-chip or free-space optical elements to spatially separate directional excitations from detection areas, the here proposed approach has obvious advantages due to the unique material performances of organic fibers. While other technologies require careful, sensitive fabrication stages, or specialisation to the specific device geometries and analyte spectral properties, exploiting polarised organic sources works with any combination of excitation and emission wavelengths, and with analytes characterised by small (<5 nm) Stokes' shift. In perspective, this approach may lead to embedding nanofibers with polarised emission at different wavelengths in the same active area, thus exciting specifically different flowing analytes at the same time. Moreover, being separated by the liquid environment because of the optically-transparent PDMS or quartz layer constituting the bottom of the fluidic microchannels, the nanofiber surface is not affected by local fluctuations in the liquid (solution concentration, flow rates, pH, *etc.*), that can be particularly important in micro- and nanofluidic environments and that can in principle deteriorate the emission properties of organic nanostructures. Differently from PLEDs, this method allows one to obtain sub-wavelength spatial resolution down to the single-fiber scale without the need for nanolithographies. Polarised emission is achieved with no need for complex devices integrating polarising elements or grating structures, which are hardly compatible with microfluidics.

The effectiveness of this approach by means of nanofibers fabricated by different organic materials needs to be assessed in depth. Organic semiconductors or dyes exhibiting high luminescence efficiency are certainly more suitable for the realisation of bright light-emitting nanostructures for chromophores excitation. Polymer molecules with luminescence absolute quantum yield up the order of 70–80% at the solid-state have been reported.[26] Experiments employing other active polymers for ES

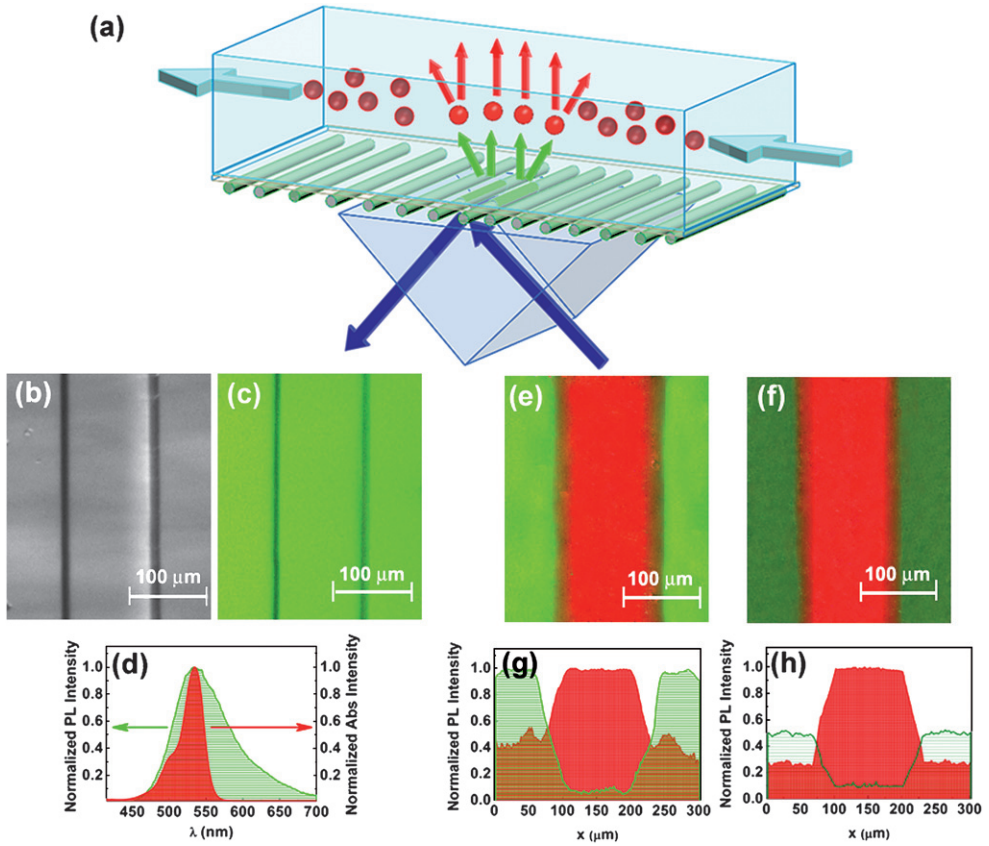

Fig. 3 Aligned arrays of active nanofibers as polarised light sources for lab-on-a-chip applications. (a): Mechanisms of operation involving a transparent substrate separating the nanofiber sources from the liquid microenvironments, where flow carries sample chromophores. Excitation of the nanofibers is performed by a TIR scheme through the schematised prism. Blue arrows indicate the excitation laser light. The light from the nanofiber arrays, being polarised, can be straightforwardly removed from the signal collected through transparent microchannels. (b–c): Optical and fluorescence micrographs of a 100 μm wide channel defined by a textured PDMS element in conformal contact with a cover slip on an aligned array of MEH-PPV-based nanofibers. (d): Nanofiber polarised emission (green spectrum, left vertical scale) and R6G absorption (red spectrum, right scale). (e–f): Decoupling of sample emission and excitation signals: R6G injected in the microchannel is excited through the green fluorescence of nanofibers (e). The signal from excitation is largely removed by rotating a polarisation analyser in front of the microscope objective perpendicular to the nanofibers longitudinal axis, which keeps almost constant the intensity of the signal from R6G (f). (g–h): S/N ratio enhancement: conjugated polymer nanofibers (green area) and R6G molecules (red area) PL intensity profiles along the microchannel cross section, without (g), and with (h) the fiber-perpendicular polariser.

nanofibers are currently in progress in our laboratories. In particular, nanofibers made by conjugated polymers[27] or embedding other molecules with optical gain would easy exhibit lasing emission, thus allowing enhanced spectral selectivity and excitation directionality.[28]

Conclusions

We realize aligned arrays of light-emitting nanofibers based on conjugated polymers by ES, and exploit the polarized emission for the photo-excitation of chromophores in prototype microfluidic channels. To this aim, we correlate the achievable degree of fiber alignment and ES parameters with the resulting optical anisotropy. Upon embedding the so-obtained active areas (up to many mm^2) in transparent microchannel geometries, we excite chromophores with a significant increase of the S/N ratio with respect to unpolarised detection. Miniaturised, organic electrospun fibers in microfluidic networks are an excellent prototype demonstrator of how exploiting together plastic light sources and lab-on-a-chip devices.

Acknowledgements

The authors are grateful to the support of the Apulia Regional Strategic Project PS_144.

References

1 L. Xia, P. Yang, Y. Sun, Y. Wu, B. Mayers, Y. Yin, F. Kim and H. Yan., *Adv. Mater.*, 2003, **15**, 353.
2 M. L. Chabinyc, D. T. Chiu, J. Cooper McDonald, A. D. Stroock, J. F. Christian, A. M. Karger and G. M. Whitesides, *Anal. Chem.*, 2001, **73**, 4491.
3 S.-W. Ahn, K.-D. Lee, J.-S. Kim, S. H. Kim, J.-D. Park, S.-H. Lee and P.-W. Yoon, *Nanotechnology*, 2005, **16**, 1874.
4 J. B. Edel, N. P. Beard, O. Hofmann, J. C. deMello, D. D. C. Bradley and A. J. deMello, *Lab Chip*, 2004, **4**, 136.
5 K. S. Shin, Y.-H. Kim, K.-K. Paek, J.-H. Park, E.-G. Yang, T.-S. Kim, J.-Y. Kang and B.-K. Ju, *IEEE Electron. Dev. Lett.*, 2006, **27**, 746.

6 B. Yao, G. Luo, L. Wang, Y. Gao, G. Lei, K. Ren, L. Chen, Y. Wang, Y. Hu and Y. Qiu, *Lab Chip*, 2006, **5**, 1041.
7 A. Pais, A. Banerjee, D. Klotzkin and I. Papautsky, *Lab Chip*, 2008, **8**, 794.
8 M. V. Kakade, S. Givens, K. Gardner, K. H. Lee, D. B. Chase and J. F. Rabolt, *J. Am. Chem. Soc.*, 2007, **129**, 2777.
9 A. Bianco, G. Iardino, A. Manuelli, C. Bertarelli and G. Zerbi, *Chem. Phys. Chem.*, 2007, **8**, 510.
10 L. M. Bellan and H. G. Craighead, *Polymer*, 2008, **49**, 3125.
11 D. Li, Y. Wang and Y. Xia, *Adv. Mater.*, 2004, **16**, 361.
12 S. Chuangchote, T. Srikhirin and P. Supaphol, *Macromol. Rapid Commun.*, 2007, **28**, 651.
13 D. Hu, J. Yu and P. F. Barbara, *J. Am. Chem. Soc.*, 1999, **121**, 6936.
14 H. Dong, V. Nyame, A. G. MacDiarmid and W. E. Jones Jr., *J. Pol. Sci.: Part B: Polymer Physics*, 2004, **42**, 3934.
15 L. Q. Liu, D. Tasis, M. Prato and H. D. Wagner, *Adv. Mater.*, 2007, **19**, 1228.
16 T. Clausnitzer, T. Kämpfe, E.-B. Kley, A. Tünnermann, A. Tishchenko and O. Parriaux, *Appl. Opt.*, 2007, **46**, 819.
17 G. H. Kim and W. D. Kim, *Appl. Phys. Lett.*, 2006, **88**, 233101.
18 Y. Ishii, H. Sakai and H. Murata, *Mater. Lett.*, 2008, **62**, 3370.
19 D. Li, Y. Wang and Y. Xia, *Nano Lett.*, 2003, **3**, 1167.
20 T. Huser, M. Yan and L. J. Rothberg, *Proc. Natl. Ac. Soc.*, 2000, **97**, 11187.
21 Z. Yu and P. F. Barbara, *J. Phys. Chem. B*, 2004, **108**, 11321.
22 C. R. L. P. N. Jeukens, P. Jonkheijm, F. J. P. Wijnen, J. C. Gielen, P. C. M. Christianen, A. P. H. J. Schenning, E. W. Meijer and J. C. Maan, *J. Am. Chem. Soc.*, 2005, **127**, 8280.
23 K. H. Lee, D. J. Kim, B. G. Min and S. H. Lee, *Biomed. Microdev.*, 2007, **9**, 435.
24 D. Yang, X. Niu, Y. Liu, Y. Wang, X. Gu, L. Song, R. Zhao, L. Ma, Y. Shao and X. Jiang, *Adv. Mater.*, 2008, **20**, 1.
25 M. Dandin, P. Abshire and E. Smela, *Lab Chip*, 2007, **7**, 55.
26 A. C. Grimsdale, K. L. Chan, R. E. Martin, P. G. Jokisz and A. B. Holmes, *Chem. Rev.*, 2009, **109**, 897.
27 F. Di Benedetto, A. Camposeo, S. Pagliara, E. Mele, L. Persano, R. Stabile, R. Cingolani and D. Pisignano, *Nature Nanotechnol.*, 2008, **3**, 614.
28 A. Camposeo, F. Di Benedetto, R. Stabile, A. A. R. Neves, R. Cingolani and D. Pisignano, *Small*, 2009, **5**, 562.

